Terminology and Strategy to Describe Large Volcanic Landslides and Debris Avalanches

Benjamin Bernard, Shinji Takarada, S. Daniel Andrade, and Anja Dufresne

Abstract

Large volcanic landslides and debris avalanches are rapid, water unsaturated, gravity-driven mass movements produced by the failure of one (or more) portion(s) of a volcanic edifice. In this chapter, we evaluated the current terminology used to describe this phenomenon. We propose a descriptive scheme based on metrics and geological features that allows us to extract significant information from both the source area and the deposit. The landslide scar is a breached depression in the volcanic edifice with steep walls, and the debris avalanche deposit is an epiclastic, unsorted, heterogeneous and heterometric breccia, composed of pieces of the edifice source, the transport path, and sometimes the basement/substratum of the volcano. Typical structures, such as jigsaw cracks and hummocky topography, along with some rarer descriptive elements are illustrated with numerous examples. This work aims to improve field analysis and remote sensing and to enhance comparative studies between different events around the world.

1 Introduction

Large volcanic landslides and debris avalanches (>0.1 km^3) are significant volcanic hazards, being directly or indirectly responsible for more than 20,000 fatalities since 1600 AD (Auker et al. 2013). For example, the recent landslide at Anak Krakatau on 22 December 2018 and subsequent tsunami caused at least 431 deaths (Williams et al. 2019). Since the Mount St. Helens event on 18 May 1980 (Voight et al. 1981), this phenomenon has become a major topic of investigation in volcanology. Hundreds of scientific articles have been published on the subject in the last four decades, along with several book chapters. Most of them use a relatively close scientific terminology but some terms such as "collapse", "caldera" and "avalanche" are ambiguous because they are also used for other volcanic phenomena that might lead to misinterpretations. Other terms such as "rockslide" and "lateral collapse" are less used inducing poor benchmarking. Nomenclature is critical in a continually evolving science such as volcanology because each scientific term must convey a message that is coherent with either the characteristics of the feature (i.e., descriptive

B. Bernard (✉) · S. D. Andrade
Instituto Geofísico, Escuela Politécnica Nacional, Ladrón de Guevara E11-253, Quito, Ecuador
e-mail: bbernard@igepn.edu.ec

S. Takarada
Geological Survey of Japan, AIST, Site 7, 1-1-1, Higashi, Tsukuba, Ibaraki 305-8567, Japan

A. Dufresne
Engineering Geology and Hydrogeology, RWTH-Aachen University, Lochnerstr. 4–20, 52064 Aachen, Germany

M. Roverato et al. (eds.), *Volcanic Debris Avalanches*, Advances in Volcanology,
https://doi.org/10.1007/978-3-030-57411-6_3

terms) or the current understanding of the physical processes (i.e., concepts). It is also relevant, in a highly productive science, to precisely define keywords to help scientists in comparative analysis. We think that now, 40 years after the paradigm shift that was the Mount St. Helens event, is an excellent time to take a hard look at the vocabulary used and propose, if necessary, changes to our language usage. We also propose a descriptive strategy using adequate terms to make field observations less subjective and enhance comparisons between different structures and deposits worldwide. In this chapter, we investigate the definition of the phenomenon before reviewing its main physical/measurable features that are the landslide scar and the debris avalanche deposit.

2 Definitions of the Phenomena

This part is mainly based on the work of Siebert (1984), Glicken (1991), and Ui et al. (2000) but also incorporate other works that deal with more specific aspects. We first present the direct and indirect observations made on the phenomena and then discuss the different terms used to define them. The most common synonyms are also presented, but the terms which best depict the features of the processes should be adopted. In the literature, most of the definitions include two parts that describe: (1) the initiation phase, and (2) the transport phase.

2.1 The Initiation Phase

2.1.1 Eyewitness, Time-Scale, Dimension, and Definition

With about 5–6 occurrences of large volcanic landslides per century since the 1600 s (Siebert and Roverato 2020), this phenomenon is scarce at a human life-time scale, so the probability of having eyewitness and measurements on an event is very low. Although, in the last four decades, volcanologists have been able to make observations with modern techniques at three occasions, namely during the Mount St Helens (USA) eruption in 1980 (Voight et al. 1981), the Soufrière Hills (Montserrat) eruption in 1997 (Voight et al. 2002), and the Anak Krakatau (Indonesia) eruption in 2018 (Williams et al. 2019). Unfortunately, both the Soufrière Hills and Anak Krakatau events occurred at night, so there are no direct eyewitnesses of these events. During the Mount St Helens event, the initiation phase was described by Stoffel and Stoffel (1980) as follows: "everything north of a line drawn east–west across the northern side of the summit crater began to move as one gigantic mass". In this event, the initiation consisted of three retrogressive and consecutive slides that removed 2.3 km^3 from the volcanic edifice (Voight et al. 1981). This description fits quite well with the observations made at the recent Anak Krakatau flank failure in which at least two failure planes were identified on a Sentinel-1A SAR image 8 h after the event (Williams et al. 2019). It is also supported by analogue models showing coherent landslide behaviour and reproducing typical landslide scar and debris avalanche hummocky topography (Shea and van Wyk de Vries 2008; Andrade and van Wyk de Vries 2010).

The study of ground deformation before the event at Mount St Helens suggests that bulging on the north flank began between March 19 and 31, and had a relatively steady rate of 1.5–2.5 m per days ($\sim$2 to 3 $\times$ 10^{-5} m/s) until May 18 (Lipman et al. 1981). On May 18, only 26 s after a magnitude 5.1 earthquake, the first slide had moved about 700 m, reaching a velocity of 40 m/s (Voight et al. 1981). The acceleration of the volcanic portion is therefore estimated, if the earthquake is the triggering mechanism, between 1.0 and 1.5 m/s^2. To separate the long-term volcanic deformation and the rapid mass movement, we can use the acceleration ($\sim$0.1 g) as a quantitative indication of the beginning of the landslide. If continuous monitoring of an active volcano is performed through real-time geophysical methods, such as real-time GPS or continuous Electronic Distance Measurements, such acceleration can be used as an early warning triggering mechanism.

Landslide volume can be of any size, ranging from 10^{-5} to 10^4 km^3 (Legros 2002; Crosta et al.

2005). Observations made in non-volcanic environments show that events smaller than one million m^3 behave as granular flows with travel distances that reflect a frictional flow regime (McSaveney et al. 2000), but this distinction is made for the transport phase, not the initiation phase. For volcanic events, some authors make a distinction between small (<0.1 km^3) and large or mega (>0.1 km^3) events that are usually related to the triggering mechanisms (Siebert 2002; Yoshida 2016). In this chapter, we focus our attention on the large events, but most of the terminology can also be used for smaller events.

Accordingly, the initiation phase can be described as the *translation, rapid and mostly horizontal, of one* (*or more*) *portion*(*s*) *composed of multiple volcanic units over a slide surface produced by a failure in the volcanic edifice* (Fig. 1; Table 1). This definition excludes phenomena such as vertical collapses (such as pit

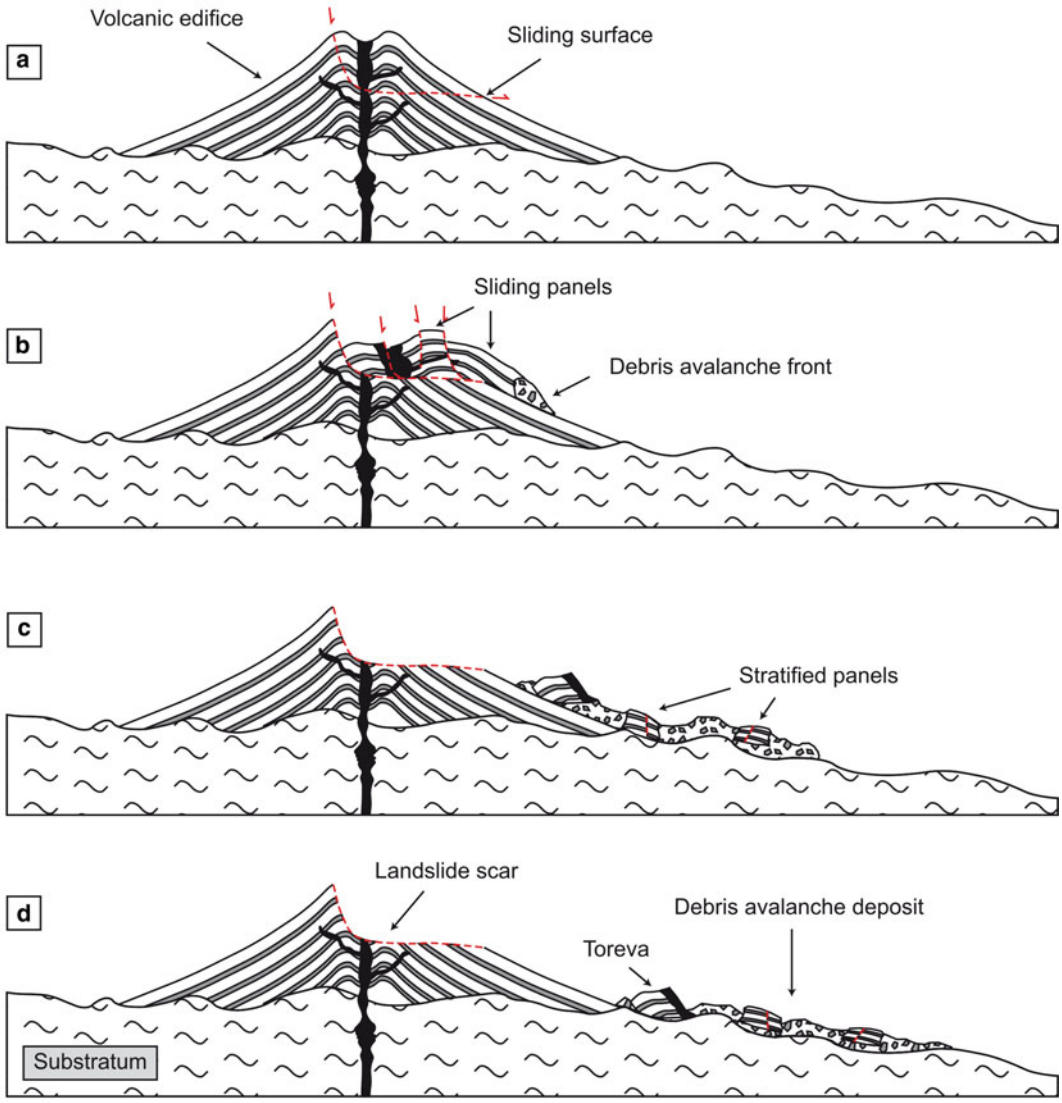

Fig. 1 Sketch of a volcanic landslide and debris avalanche with **a** the initial state; **b** the initiation; **c** the transport; and **d** the final state. Modified from Bernard (2008)

Table 1 Definition and terms used to describe large volcanic debris avalanches

Phase	Definition	Preferred term	Synonyms	Field evidence (Sects. 3 and 4)
Initiation	Translation, rapid and mostly horizontal, of one (or more) portion(s) composed of multiple volcanic units over a slide surface produced by a failure in the volcanic edifice	Volcanic landslide	Sector collapse, lateral collapse, flank collapse, rockslide, slope failure, flank failure	Breached depression in the volcanic edifice with steep walls (volcanic landslide scar)
Transport	Rapid water-unsaturated gravity-driven mass movement of multiple volcanic units	Volcanic debris avalanche	Rockslide avalanche, Rockslide-debris avalanche	Epiclastic, unsorted, heterogeneous and heterometric breccias with a hummocky surface, composed of pieces of the edifice source and the transport path (volcanic debris avalanche deposit)

and caldera collapses), rock falls, and long-term volcanic deformation such as creeping or spreading.

2.1.2 Terminology

The most popular term used to name the initiation phase is probably "sector collapse" (Boudon et al. 1987; Kokelaar and Romagnoli 1995; Richards and Villeneuve 2001; Ponomareva et al. 2006; Bernard et al. 2008; Kervyn et al. 2008; Delcamp et al. 2016) which highlights the fact that the failure removes away "a sector" of the volcano. Nevertheless, this term is ambiguous as it can be confused with partial vertical collapse. In order to distinguish this rupture from a purely vertical collapse and to specify that the mass movement is toward one particular direction, several authors proposed the terms "lateral collapse" (Marti et al. 1997; Day et al. 1999; Tibaldi et al. 2006; Romagnoli et al. 2009) and "flank collapse" (Vincent et al. 1989; Day et al. 1997; Elsworth and day 1999; Leyrit 2000; Le Friant et al. 2004; Arce et al. 2008; Andrade and van Wyk de Vries 2010; Macías et al. 2010). Capra et al. (2002) and Scott et al. (2005) distinguish "sector collapse" from "flank collapse", suggesting that the latter is typically smaller and does not involve the volcano summit and core. Some authors prefer the term "rockslide" because it takes into account the description of the rupture. This term was first used to describe the Mount St. Helens event (Voight et al. 1981) and has also commonly been used ever since (McEwen et al. 1989; Cruden and Lu 1992; Glicken 1996; Shea et al. 2008; Paguican et al. 2014). However, the definition of a rockslide, as taken from the slope movements classification (Varnes 1978; Hungr et al. 2014), implies the slide of (multiple) rock units, but a volcanic edifice is made of both massive rock units (lavas) and loose volcaniclastic and epiclastic formations. The terms "slope failure", "flank failure", "slope instability", and "flank instability" have been frequently used for volcanic islands or submarine events (Johnson 1987; McGuire 1996; Hürlimann et al. 2000; Lipman et al. 2003; Coombs et al. 2007; Paris et al. 2011; Williams et al. 2019), but could relate to longer-term mass wasting processes such as creeping. We considered that the best term describing the initiation phase is probably "volcanic landslide" (Duffield et al. 1982; Stoopes and Sheridan 1992; Iverson 1995; Carracedo et al. 1999; Legros et al. 2000; Hürlimann et al. 2000; Watt et al. 2009; Delcamp et al. 2017) since it includes the dynamic aspect (slide) and the material involved (volcanic land) without being too specific. The rupture can involve or not the volcano summit and may be caused by different edifice weakening processes and triggering mechanisms. Volcanic landslides might also provoke various secondary phenomena such as directed blast, debris flow, or tsunami

(Siebert et al. 1987). In the field, the evidence of a volcanic landslide is a breached depression with steep walls at the source (Fig. 1).

2.2 The Transport Phase

2.2.1 Eyewitness, Time-Scale, Dimension, and Definition

Very few direct observations exist on the transport phase of this phenomenon. During the Mount St. Helens event, this stage was hidden by the lateral blast cloud created by the rapid decompression and explosion of the cryptodome (Stoffel and Stoffel 1980). Emplacement times of less than 3 min and about 10 min have been estimated for Soufrière Hills (runout 4 km) and Mount St Helens (runout 26 km) events, respectively. Velocity values obtained by measurements or calculations are generally between 20 and 100 m/s (Voight et al. 1981, 2002; Siebert et al. 1987). These mass movements can travel a long distance (up to 10 s of km) and affect considerable area (up to 100 s of km^2) (Siebert 1984; Ui et al. 2000). Transport mechanisms are generally studied through deposit analysis, but the emplacement mode remains highly controversial (Ui et al. 2000). However, it is possible to give a general description of the transport phase as a *rapid water-unsaturated gravity-driven mass movement of multiple volcanic units* (Fig. 1; Table 1). This definition excludes other volcanogenic flows such as lava flows, pyroclastic density currents, and lahars.

2.2.2 Terminology

Most of the authors use the term "debris avalanche" for the transport phase (Crandell et al. 1984; Glicken 1991; Hayashi and Self 1992; Ui et al. 2000; van Wyk de Vries and Delcamp 2015). This term may sometimes be employed to imply a certain degree of the incoherence of a flow made of debris (Fisher et al. 1987). There is widespread evidence in the deposits showing that a significant part of the mass moves in a nearly coherent manner, for example, the presence of toreva (Belousov et al. 1999; van Wyk de Vries et al. 2001; Clavero et al. 2002; Roa et al. 2003; Bernard et al. 2011; see Sect. 4 for definition) and large panels with original stratigraphy preserved even several tens of kilometers away from the source (Glicken 1991; Takarada et al. 1999; Bernard 2008; Fig. 2). To illustrate these characteristics, some authors prefer the terms "rockslide avalanche" (Voight et al. 1981; Shea et al. 2008) and "rockslide-debris avalanche" (Glicken 1996; Paguican et al. 2014). Studies of those deposits show that a layer, containing elements from both the landslide source and the substratum, is formed at the base of the moving mass due to intense shearing and mixing (Schneider and Fisher 1998; Takarada et al. 1999; Bernard et al. 2008) so the basal contact is mainly not a slide surface. Exceptions exist, such as the 8 ka Parinacota deposit (Chile), where some blocks have slid several 10 s of meters away from the main deposit body due to a slippery fluvio-lacustrine substratum (Clavero et al. 2002). To have a consistent terminology, we propose to use the term "volcanic debris avalanche" that best describes the transport phase. In the field, the evidence of a debris avalanche is a hummocky deposit at the foot of the volcano (Fig. 1).

3 Descriptive Strategy for the Volcanic Landslide Scar

3.1 Terminology

In the literature, the most common morphological term used to describe this structure is "caldera," preceded by a genetic qualifier such "sector collapse" or "avalanche" to distinguish it from collapse caldera (Siebert 1984). Nevertheless, "caldera" derives from the Spanish word "Caldero" (cauldron in English, caldeirão in Portuguese) and depicts a sub-circular depression with vertical walls and an almost flat, horizontal floor. This term accurately illustrates structures formed by vertical collapse due to large ignimbrite eruption (e.g., Crater Lake caldera, USA) or large basaltic lava outpouring (e.g., Mokuaweoweo caldera at Mauna Loa, Hawaii) but does not fit the description of the volcanic landslide rupture zone that is opened in the

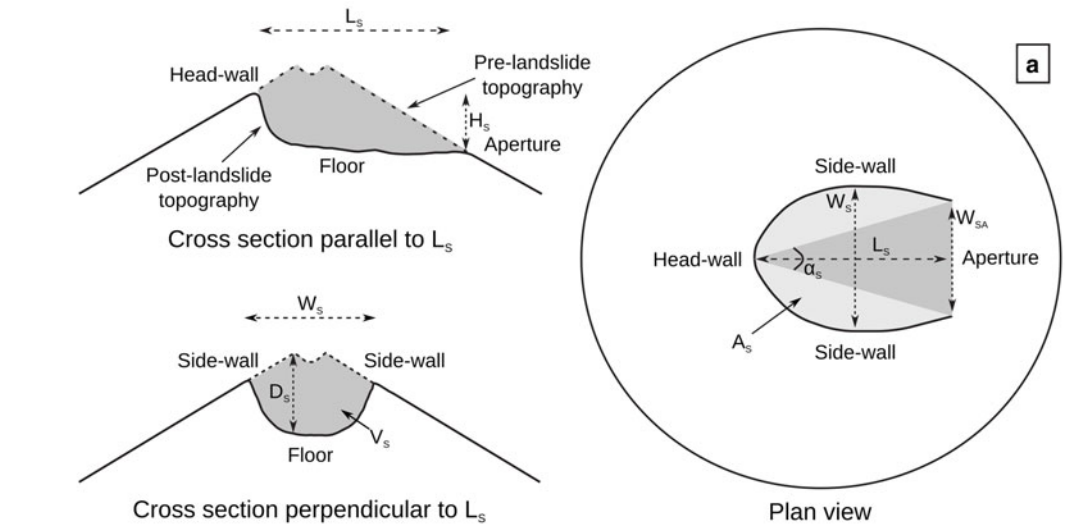

Fig. 2 Descriptive elements and dimensions for a volcanic landslide scar. **a** Cross-sections and plan view with the main descriptive terms and geometrical parameters defined in Table 2. **b** Mayuyama landslide scar, Japan

direction of the landslide. The terms "horseshoe-shaped" or "U-shaped caldera" have been commonly used to distinguish the volcanic landslide source from the other vertical structures (Siebert et al. 1987, van Wyk de Vries and Delcamp 2015). Some authors prefer the term "collapse amphitheater" (Ui et al. 2000; Coombs et al. 2007) and use it to describe some of the most typical rupture structure (e.g., Mount St Helens, USA) but "amphitheater" might not be an adequate term as it refers to a circular or elliptical open-air venue (e.g., Colosseum amphitheater in Rome). In the literature concerning non-volcanic landslides, the terms "scar" and "scarp" have

been used interchangeably but some authors (Strasser and Schlunegger 2005; Yoshimatsu and Abe 2006) propose that a scar is a mark left by a rupture whereas a scarp is a steep slope formed by various processes such as faulting, erosion or deposition (e.g., scarps form a high viscosity lava front). The term "scar" has already been used in the volcanic context (Oehler et al. 2008; Shea et al. 2008; van Wyk de Vries and Delcamp 2015), and we consider that the best term to depict the source should be "volcanic landslide scar." The depression formed during a volcanic landslide can thus be described using three geomorphological elements (Fig. 2): (1) the "wall", which corresponds to the steep limit of the scar; (2) the "floor", which stands for the relatively flat, but not necessarily horizontal, the interior of the depression; and (3) the "aperture", which is the region between the lowermost points of the wall. We may differentiate the "head-wall", that faces the aperture of the depression (Siebert 1984), and the "side-walls", which are more parallel to the general landslide direction. Thus, the aperture can be defined as the section between the side-walls' extremity.

3.2 Metrics

The morphology of the rupture zone can be described using common metrics presented in Fig. 2a and defined in Table 2 (Siebert 1984; Legros 2002; Bernard 2008; Dufresne 2009). The scar evolves through time due to subsequent erosion of the wall and to filling of the depression by the material of different origin (e.g., post-landslide volcanic activity, glacial erosion, rockfall from the walls) so the reconstruction of the original scar size might be the result of an interpretative work based on geologic and topographic data. Thus, any parameter estimated or measured after interpretation must be moderated with a margin of error (Siebert et al. 2004; Yoshida and Sugai 2007; Bernard et al. 2008). To compare scars of different sizes, we propose to complete their description with dimensionless parameters such as elongation, aspect ratio, and closure factors (Table 2).

3.3 Morphology

The description of the landslide scar is generally done using plan view and profile representations. In plan view the terms "horseshoe", "amphitheater", and "U-shaped" are typical (Siebert 1984; Belousov et al. 1999; Ui et al. 2000; Riggs and Carrasco-Nunez 2004) completed by terms like "deep-seated" and "thin-skinned" in cross-sections to denote the depth of the failure (Siebert 1984; Petley and Allison 1997; Coombs et al. 2007). Horseshoe scars have an aperture width smaller than their maximum width (e.g., Mayuyama scar; Siebert et al. 1987). Amphitheater scars are described as semi-circular structures. However, this term might not be etymologically correct (see Siebert and Roverato 2020, this volume) and, therefore, we propose to use "semi-circular" as a descriptive term for such structure that is also characterized by its width being close to twice its length (e.g., Duau scar; Johnson 1987). U-shaped scars have a semi-circular head-wall and parallel side-walls, and their length is generally larger than their width (e.g., Reventador 19 ka scar, Bernard and Andrade 2019). Triangular scars in plan view, such as the one at Socompa (van Wyk de Vries et al. 2001), are scarcer with clearly divergent linear side-walls. Deep-seated structures, such as Mount St. Helens landslide scar, generally have steep high walls and an almost horizontal floor while thin-skinned structures, such as Mayuyama one (Ozeki et al. 2005), have much steeper floors and smaller walls (Fig. 3). Irregular scars, such as Guagua Pichincha (Robin et al. 2010), are also frequent, in particular in compound volcanoes and volcanic complexes.

The analysis of the scar shapes could be used to understand the long-term weakening process, short-term instability, and triggering mechanisms. Deep-seated scars are frequently associated with deep processes such as cryptodome intrusions (Siebert 2002) or highly altered volcano cores (Bernard 2008), whereas thin-skinned scars are generally associated with external processes such as heavy rainfall (Kerle and van Wyk de Vries 2001). Triangular and large U-shaped scars can be created when the failure initiates in

Table 2 Definition of the quantitative parameters for the volcanic landslide scar

Acronym	Descriptive parameter	Definition
L_S	Scar length	Distance from the head-wall to the middle of the aperture
W_S	Scar width	Maximum distance between the side-walls, orthogonal to the length
W_{SA}	Scar aperture width	Distance between the side-walls at the aperture
H_S	Scar height	Height between the top of the head-wall and the aperture
α_S	Scar aperture angle	Angle between the lines drawn from the head-wall to the side-walls extremity
β_S	Scar slope	Slope between the top of the head-wall and the aperture (β_S = atan H_S/L_S)
γ_S	Scar azimuth	Azimuth of L_S
A_S	Scar area	Surface of the scar in plan view
D_S[a]	Scar depth	Maximum depth of the scar between the pre and post-landslide topography
V_S[a]	Scar volume	Volume difference before and after the landslide
T_S[a]	Scar thickness	Average thickness ($T_S = V_S/A_S$)
AR_S	Scar aspect ratio	Ratio between the average thickness and the radius of a circle of equal area ($AR_S = T_S/\sqrt{(A_S/\pi)}$)
EF_S	Elongation factor	Ratio between the scar length and width ($EF_S = L_S/W_S$)
CF_S	Closure factor	Ratio between the scar aperture width and the scar width ($CF_S = W_{SA}/W_S$)

[a]Parameters with a large error if pre- or post-landslide topographies are poorly known

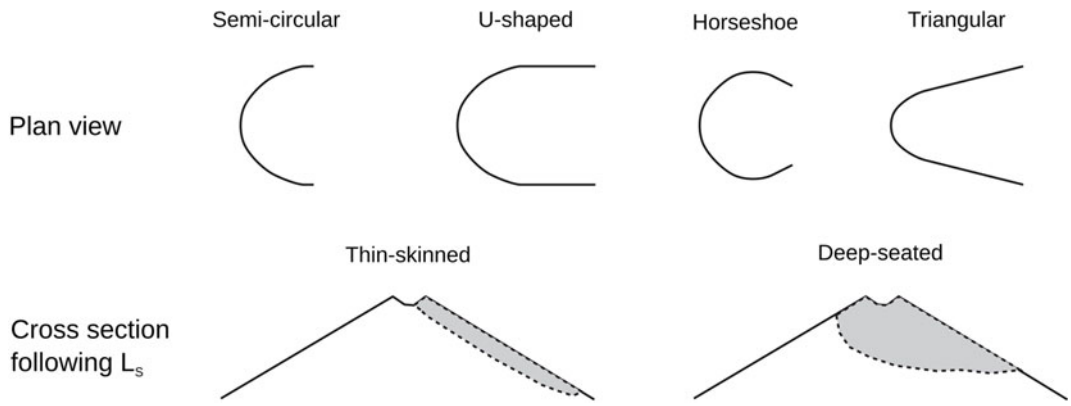

Fig. 3 Common shape of volcanic landslide scar in plan view and cross-section

or propagates to the volcanic substratum/basement (van Wyk de Vries et al. 2001), whereas horseshoe scars are usually associated with eruptions (Voight et al. 1981). Nested scars associated with recurrent volcanic landslides are also a common feature that can influence the shape of the scar (Belousov et al. 1999; Bernard and Andrade 2019). Nevertheless, no systematic relationship has yet been presented between the shape of the landslide scar and its origin. Such a study should be considered as highly relevant in the future.

3.4 Geological Elements and Distinction from Other Volcanic Depressions

To study the origin of the landslide, a geological description of the scar is necessary. Structural elements such as dikes and faults intersecting the walls can provide insights into local stress regime and might be related to the direction of aperture (Siebert 1984; Lagmay et al. 2000; Paguican et al. 2012; Andrade et al. 2018). Long-term weakening processes and instability factors can also be assessed when studying the nature and physical and chemical alteration of the wall units (Voight et al. 2002; Oehler et al. 2008; Roverato et al. 2020, this volume).

Volcanic landslide scars can be distinguished from most other volcanic depressions due to their shape and their dimensions (Siebert 1984). Evidence of an aperture is a major criterion to differentiate them from collapse calderas or craters, but sometimes those can be breached by eruptions or erosion processes. Nonetheless, those secondary apertures tend to be much narrower compared to landslide scar apertures and could be discriminated using the closure factor (Table 2). The aperture can also be hidden by following eruptive activity, and then more geological and geophysical investigations are required. Glacial erosion structures, such as glacial cirques, can also look like landslide scars but are generally shallower and filled with glacial deposits (Karátson et al. 1999). Fluvial erosion can be assessed through the analysis of the shape and depth of the fluvial network (Paris and Carracedo 2001).

4 Descriptive Strategy for the Volcanic Debris Avalanche Deposit

4.1 Terminology of the Fundamental Elements

The volcanic debris avalanche deposits (VDAD) are epiclastic, unsorted, heterogeneous, and heterometric breccias composed of pieces of the edifice source and the transport path (Siebert 1984; Glicken 1991; Ui et al. 2000; Leyrit 2000). Such deposits have multiple facies and complex structures, hence the terminology used to describe them has become somewhat confusing. The component terminology in volcanic or non-volcanic debris avalanche deposits is a controversial subject that has led to an extensive literature (Ui 1983; Ui and Glicken 1986; Glicken 1991; Palmer et al. 1991; Yarnold 1993; Friedmann 1997; Belousov et al. 1999; Takarada et al. 1999; Nehlig et al. 2001; Shea et al. 2008).

Glicken (1991) distinguishes two kinds of fundamental elements: clasts and debris avalanche blocks (Fig. 4). This distinction has been used almost unanimously ever since. A clast is defined as "rock of any size that would not break if passed through a sieve or immersed in water".

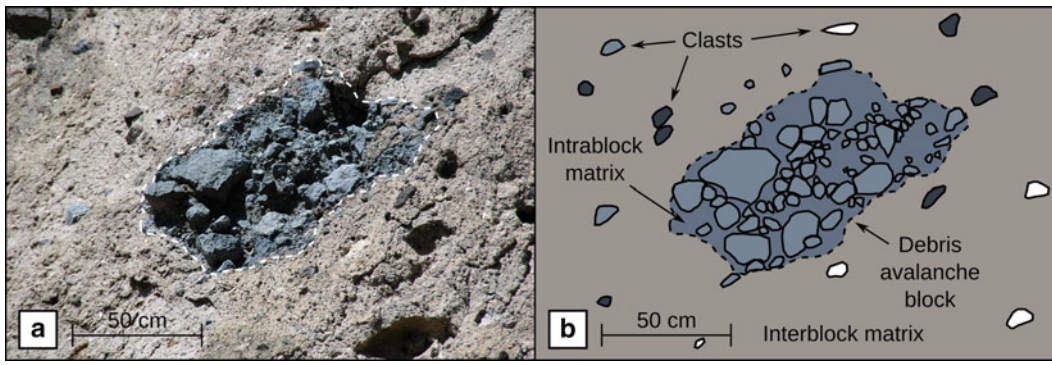

Fig. 4 Volcanic debris avalanche deposit descriptive elements. Photo **a** and drawing **b** of an outcrop from the 2.4 Ma Mont Dore VDAD, France. Modified from Bernard (2008)

Except for particularly fragile particles such as prismatically jointed blocks, this term is unequivocal. A debris avalanche block (DAB) is defined as "an unconsolidated (or poorly consolidated) piece of the old mountain transported (?) to its place of deposition". The definition mentions that all DABs come from the source-edifice, but it has been undoubtedly verified that large coherent portions of VDADs are made of substratum material (Palmer et al. 1991; Belousov et al. 1999; van Wyk de Vries et al. 2001; Clavero et al. 2004). This term can be employed in the sense of Glicken (1991) terminology, but it should be mentioned that DABs may also be derived either from the transport path or the edifice substratum. DABs are commonly found in other deposits such as secondary slides and cohesive lahars (Capra and Macías 2000; Bernard et al. 2009), which helps to assess their primary source.

When describing large pieces of the edifice source in the deposit, some authors use the terms "megablock" or "megapanel" that can preserve their original bedding (Ui 1983; Mehl and Schmincke 1999). The minimum size and the dimension (great axis length, surface, and volume) used to describe them can vary from one author to another. These terms can look appealing, but they are redundant with the term DAB, which has no upper size limit.

The term "matrix" should be employed in its sedimentological meaning that refers to the fine grains between the larger particles (Mehl and Schmincke 1999). Glicken (1996) distinguishes the intraclast matrix (inside one particular DAB, often monolithologic) and the interclast matrix. According to the definitions of clast and DAB mentioned above, the terms "intraclast" and "interclast" should be replaced by "intrablock" and "interblock", respectively (Fig. 4). It might be of interest to distinguish the intrablock matrix present at the source and the intrablock matrix produced during transport through shattering of the debris avalanche blocks or shearing at the basal contact. Although such distinction is complicated for reworked deposits with pre-existent matrix (e.g., in autobreccia, pyroclastic, and epiclastic deposits), it could be easily done for initially massive units such as lava flows. The study of the interblock matrix and its components could help to understand the evolution of the avalanche downstream and bulking processes.

4.2 Deposit Facies

VDADs have the particularity of presenting a greater diversity of facies than any other volcanic deposit. Their description is fundamental in deciphering the complexity of this phenomenon. The variety of rock types, structures, and textures observed in VDADs is responsible for the multiplication of facies terms in the literature: block facies (Ui 1983), matrix facies (Ui and Glicken 1986), mixed facies (Glicken 1991), marginal facies (Palmer et al. 1991), sheared facies (Mehl and Schmincke 1999), bulldozer facies (Belousov et al. 1999), basal facies (Ui et al. 2000), hybrid facies (Roverato et al. 2011) and others (see Dufresne et al. 2020, this volume). Despite several attempts to build coherent terminologies, it remains difficult to compare the facies observations made in different deposits by different authors. Facies must be described more precisely to get meaningful information on the landslide origin and the flow mechanisms. A facies is generally defined by a unique character that distinguishes one rock-body from another (Cas and Wright 1987). In the following sections, we propose to split the facies analysis of VDADs into two stages that provide different information on the event.

4.2.1 First-Order Classification

Based principally on the work of Glicken (1991, 1996), we propose to use a first-order classification that allows distinguishing the mostly intact material and the newly formed material, which would be the block facies and mixed facies, respectively. Although there is a wide range of intermediate facies between them, these terms are the most widely used and are useful for mapping purposes (e.g., Bernard et al. 2008). To improve the relevance of this classification, we propose to add an adjective to the block facies to separate the material coming from the volcanic

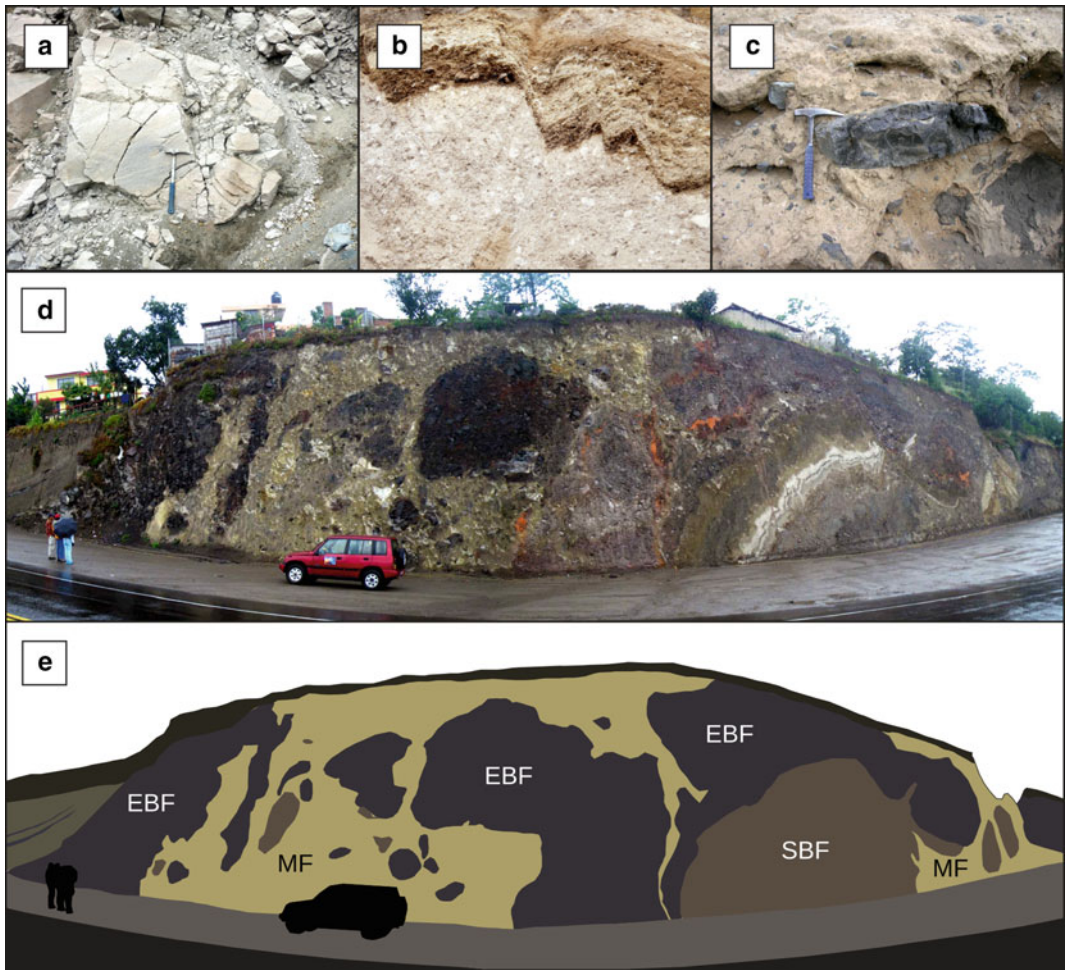

Fig. 5 Typical facies of volcanic debris avalanche deposits. **a** edifice-block facies (EBF) with jigsaw cracks from the 4.5 ka Cotopaxi VDAD, Ecuador. **b** substratum-block facies (SBF) made of Toya ignimbrite and associated reworked parts from the 20 ka Zenkoji VDAD, Japan. **c** mixed facies (MF) with a prismatic jointed block from the 60–65 ka Chimborazo VDAD, Ecuador. **d**, **e** Combination of facies from the > 30 ka Imbabura VDAD, Ecuador

edifice from the material coming from the substratum if possible (Bernard 2008).

The edifice-block facies (EBF) is almost exclusively made of material from the landslide source and is comparable to the original definition of the block facies in Glicken (1991). The EBF is made of the apposition of DABs from ancient layers of lava flows, pyroclastic density current, and fall deposits, and even epiclastic material such as debris-flow and moraines deposits (Fig. 5a). The result is a coherent unconsolidated or poorly consolidated facies with low interblock matrix that can be stratified or not, depending on its origin and the exposure size. It can be highly deformed or just a little shattered. Jigsaw cracking is a common feature in this facies. It is generally polylithological but can appear monolithological, depending on the outcrop size.

The substratum-block facies (SBF) is made of DABs coming from the transport path or the edifice basement that have been incorporated almost intact in the debris avalanche (Fig. 5b). The amount of interblock matrix is generally

higher compared to the EBF. This facies is partially similar to the bulldozer facies of Belousov et al. (1999). It generally appears at the base or the front of the VDAD but can also be fluidized and incorporated up to the top of the deposit (Bernard et al. 2008). The SBF can be made of sedimentary, volcaniclastic, and epiclastic deposits, even soil. In some cases, it can also include basement material such as altered leucogranite (Schneider and Fisher 1998). The coherence of this facies depends on the material incorporated. The degree of deformation in the SBF is extremely variable, but folding and faulting are particularly common. The distinction between SBF and EBF facies can be difficult when the former is made of volcaniclastic or epiclastic material. Good knowledge of the edifice and substratum nature can help to distinguish between them. In the case of failures due to a weak substratum, the SBF can represent most of the VDAD (van Wyk de Vries et al. 2001).

The mixed facies (MF) was defined by Glicken (1991) and referred to the completely mixed part of the VDAD, where the material has lost its original primary structures (e.g., stratifications). MF is mostly made of interblock matrix and is generally highly polylithological, light-brown colored, sometimes consolidated, unsorted, and unstratified (Fig. 5c). It may contain juvenile material and wood fragments. MF is highly heterometric. It may be possible to distinguish between the elements coming from the source edifice and the substratum when there are distinct differences such as geochemical character and clast shape (e.g., pebbles are more likely coming from the substratum). Due to their shared characteristics, MF can be confounded with landslide-triggered cohesive lahars. Detailed investigation of the internal structures, such as trapped air bubbles, can help distinguish between them (Bernard et al. 2009).

A single outcrop might expose all the facies at once (Fig. 5d, e). The quantification of each facies helps to estimate the original landslide volume, the amount of erosion, and total volume increase during transport.

4.2.2 Lithology

This part is based on the work of Cas and Wright (1987) on facies analysis. The lithological description may include the physical constituents (lava, pyroclastic, autoclastic, epiclastic, and non-volcanic; Fig. 6), their composition (geochemical, mineralogical, and petrological characters) and their texture (grain size, sorting, rounding, shape, and fabric). The identification of physical constituent can sometimes be complicated in high-deformation zones. Nonetheless, it is required for any textural analysis intended to explore the flow dynamics because the origin of the material and its primary texture influence the final texture. The physical constituent analysis also permits to study the origin of the landslide. The composition analysis is particularly interesting in two cases. If the source zone is still exposed, a comparison between the compositional maps of the scar and the deposit can provide valuable information on the emplacement processes (Kelfoun et al. 2008). If the source region is hidden, the composition analysis can

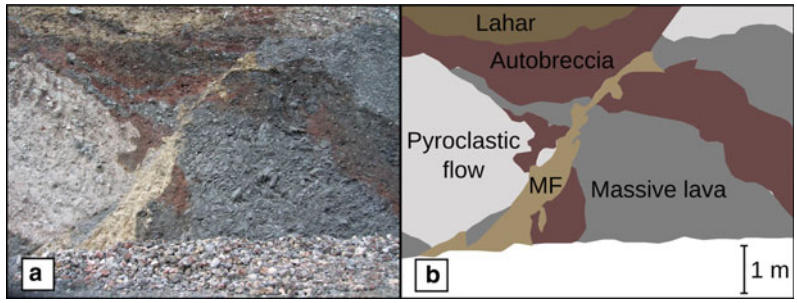

Fig. 6 Photo **a** and sketch **b** of an outcrop of the >30 ka Imbabura VDAD with facies lithologies. Modified from Bernard (2008). MF: mixed facies

help to understand the development of the volcano before the failure. A complete lithological description gives information on the volcano history, the pre-collapse state, the triggering mechanism, and the transport path nature.

4.3 Deposit Structures

The most typical structures used to identify a VDAD are jigsaw cracks (Fig. 5a) and hummocky topography (Ui 1983; Siebert 1984). These features also occur in non-volcanic rock avalanches (Dufresne et al. 2016 and references therein). Nonetheless, the variety of observed structures is much more comprehensive (Glicken 1991). In VDADs, there are innate structures such as magmatic joint, stratification, and prismatically jointed blocks. Structures existed in the volcanic edifice, before the failure, such as fractures due to tectonic stress or mechanical weathering. Additionally, there are structures acquired during the event, and finally, others developed after the deposition, due to faulting or reworking. It is essential to distinguish among those structures during fieldwork. The literature on VDAD structures is extensive and is presented here in three complementary sections: the basal contact, the internal structures, and the surface morphology.

4.3.1 Basal Structures

Even if debris avalanches, either volcanic or non-volcanic, are highly erosive (Yarnold 1993), basal contact descriptions are scarce in the literature. Some authors use the term "sole" to describe a particular space placed between the unaffected substratum and the VDAD body (Schneider and Fisher 1998). This space seems to concentrate the most extreme features from flat contact without particular structures (Clavero et al. 2002; Fig. 7d), highly deformed DABs (Fig. 7a, b), up to the occurrence of frictionite (Legros et al. 2000). Abrasion features such as striae and channels are described (Schneider and Fisher 1998; Mehl and Schmincke 1999) as well as deformation structures such as boudinage, folding, and shearing of the substratum (Clavero et al. 2004; Bernard et al. 2008). It is possible to observe wood pieces incorporated in the VDAD and oriented slightly parallel (Belousov 1995; Takarada et al. 1999) or perpendicular (Bernard et al. 2009) to the flow direction. Substratum injections in the deposit body are also observed (Bernard and van Wyk de Vries 2010; Fig. 7c). Fine-grained injections descending from the VDAD down into the substratum are more rarely observed (Schneider and Fisher 1998).

It is important to note that most of the VDAD particular facies (e.g., sheared facies, basal facies, and bulldozer facies) are related to the

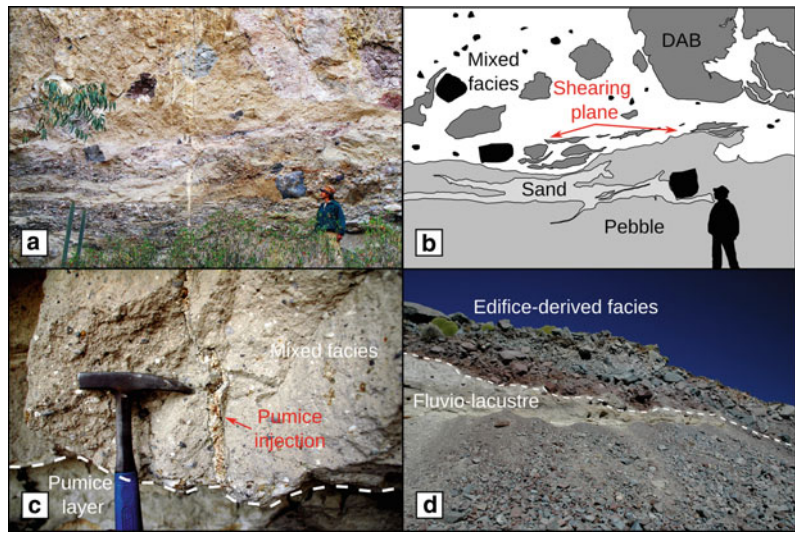

Fig. 7 Examples of basal contacts. **a**, **b** sheared basal contact in the 60–65 ka Chimborazo VDAD, Ecuador (modified from Bernard et al. 2008). **c** undulating contact with substratum injection (pumice) in the 2.4 Ma Mont Dore VDAD, France. **d** almost planar contact in the 8 ka Parinacota VDAD, Chile

incorporation of the substratum in the deposit (Friedmann 1997; Belousov et al. 1999) which can contribute to a large proportion of the total deposit volume (Palmer et al. 1991; Clavero et al. 2004). Sometimes, the whole base of the VDAD is composed of substrata incorporated during failures, such as Socompa and Mombacho examples (van Wyk de Vries et al. 2001; Shea et al. 2008).

4.3.2 Internal Structures

The most common and most described internal structure is the jigsaw cracking (Ui 1983; Fig. 8a) that corresponds to a chaotic fracture network characterized by small displacements of the resulting fragments and associated with the dilation without disaggregation of a rock unit initially not fractured (Glicken 1996). These fractures are observed at all scales (Komorowski et al. 1991; Belousov et al. 1999; Roverato et al. 2015), and they are present from the proximal to the distal part of the VDAD and can change from jigsaw crack (cracks without intrablock matrix) to jigsaw fit (open cracks with intrablock matrix) (Ui and Glicken 1986; Ui et al. 1986). It is common to observe the superimposition of jigsaw cracking over innate or acquired fractures, such as thermal and tectonic fractures, but it is quite easy to differentiate among them because jigsaw cracking is generally much more random.

There are many more internal structures in VDADs, including the following non-exhaustive

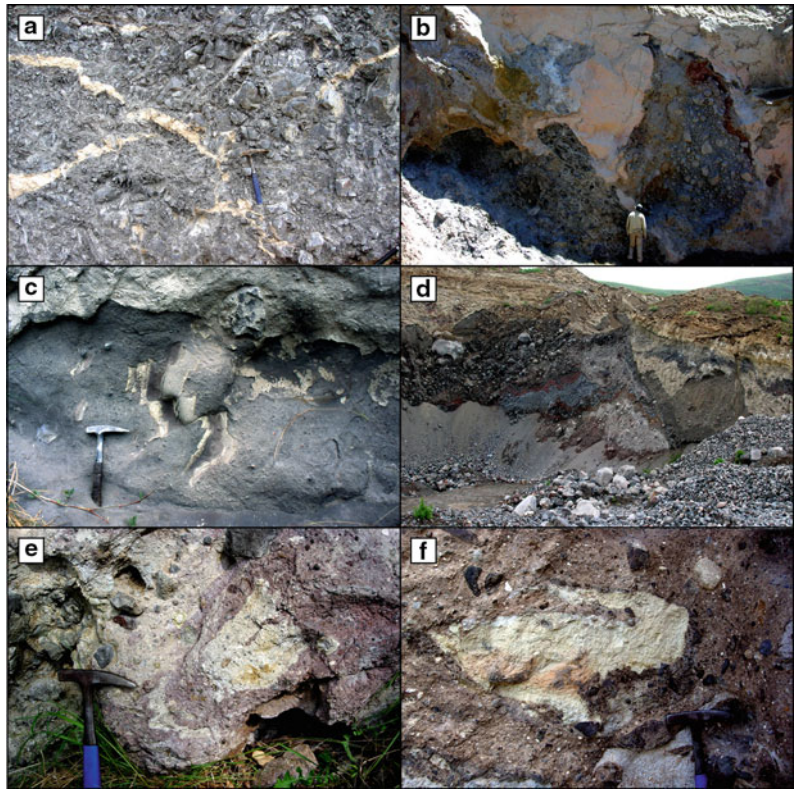

Fig. 8 Examples of internal structures. **a** jigsaw cracking and mixed facies injection in a DAB in the >30 ka Imbabura VDAD, Ecuador. **b** mixed facies and fluidized substratum injections in the 60–65 ka Chimborazo VDAD, Ecuador. **c** faulting in lacustrine deposits incorporated in the 30 ka Tungurahua VDAD, Ecuador. **d** boudinage of pyroclastic units in the >30 ka Imbabura VDAD, Ecuador. **e** mingling structure between different colour matrices in the 2.4 Ma Mont Dore VDAD, France. (**f**) vortex structure of a substratum DAB in the 2.4 Ma Mont Dore VDAD, France

list of the most common structures. These structures can also help to distinguish VDAD from other volcanoclastic or epiclastic deposits.

- Mixed facies and fluidized substratum injections in DABs (Fig. 8a, b);
- Faulting or boudinage of stratified units due to stretching of the avalanche mass (Fig. 8c, d);
- Mingling between different color matrix/facies (Fig. 8e);
- Vortex structure of DABs due to shearing (Fig. 8f);
- Impact features on block surface associated with the vibration and collision of the blocks during transport (Clavero et al. 2002);
- Hackly texture on millimeter size grains that are similar to microscopic-scale jigsaw cracks (Komorowski et al. 1991; Belousov et al. 1999);
- Ramp structure similar to thrusting (Schneider and Fisher 1998).

4.3.3 Topography

One of the most prominent features of VDADs is their characteristic surface morphology called "hummocky topography" made of widespread fields of hills (hummocks) and depressions (Siebert 1984; Fig. 9). The geomorphological term "hummock" is also used for the description of massive ice bodies and cryoclastic formations (Grab 2005). Hummock shapes and sizes are highly variable. For example, at Cotopaxi volcano, hummocks from the 4.5 ka VDAD range from less than 4 m high and 100 m^3 in volume up to 190 m high and 18 million m^3 (Encalada and Bernard 2018; Fig. 9f, h). Some hummocks have a rounded base, and their slope slowly decreases towards their summit (Crandell et al. 1984; Fig. 9b, f) while others are more conical with a constant slope and a limited summit area (Siebert 1984; Fig. 9a). Some hummocks also have polygonal bases and are called pyramidal hummocks, while others have complex irregular shapes (Fig. 9f). When hummocks are strongly elongated, they are often called ridges (Fig. 10e) and can be kilometer-long (Siebert 1984; Fig. 9c). The major ridge axis can be parallel (longitudinal ridge) or perpendicular (transversal ridge, Fig. 9g) to the flow direction (Bernard et al. 2008; Kervyn et al. 2008; Dufresne and Davies 2009; Dufresne et al. 2010). Border ridges or natural levees can mark the limits of the deposit (Ui et al. 2000). Hummocks can be qualified as "torevas" when they correspond to very large (up to >1 km-long) almost intact pieces of the landslide source that had only suffered a relatively short translation from the source and, sometimes, a slight rotation through a horizontal axis (Reiche 1937; Fig. 9d, e, h). Some torevas do not go further than the landslide scar aperture (van Wyk de Vries et al. 2001; Bernard et al. 2011), but others reach the foot of the volcanic edifice (Belousov et al. 1999). The bedding in torevas is generally inclined toward the volcano (Clavero et al. 2002). In some cases, torevas were previously interpreted as lava domes (Bernard et al. 2011).

It is typically possible to identify hundreds to thousands of hummocks on a single deposit (Crandell et al. 1984; Conway et al. 1992; Clavero et al. 2004; Shea et al. 2008; Encalada and Bernard 2018). Glicken (1991) proposes a classification based on their representative facies which we modify slightly using the facies classification proposed in this chapter (Sect. 4.2.1): (a) EBF hummocks (Siebert et al. 2004); (b) MF hummocks with a DAB core (Glicken 1991); (c) MF hummocks (Crandell et al. 1984); (d) SBF hummocks (Clavero et al. 2002). In some cases, like Parinacota or Mombacho VDADs, an evolution of the hummocks type from the proximal (mostly type a) to the distal area (mostly types c and d) is described (Clavero et al. 2002; Shea et al. 2008). Clavero et al. (2002) also distinguish between individual and compound hummocks, the latter being formed by the amalgamation of individual hummocks. The spatial organization and distribution of surface morphologies is a controversial theme, but recent analogue modeling has improved our understanding of these structures. In general, they are interpreted as the results of extension and compression of the avalanche body during transport (Shea et al. 2008; Paguican et al. 2014), and its lithology probably influences the hummock shape and size. In the field, the hummocky

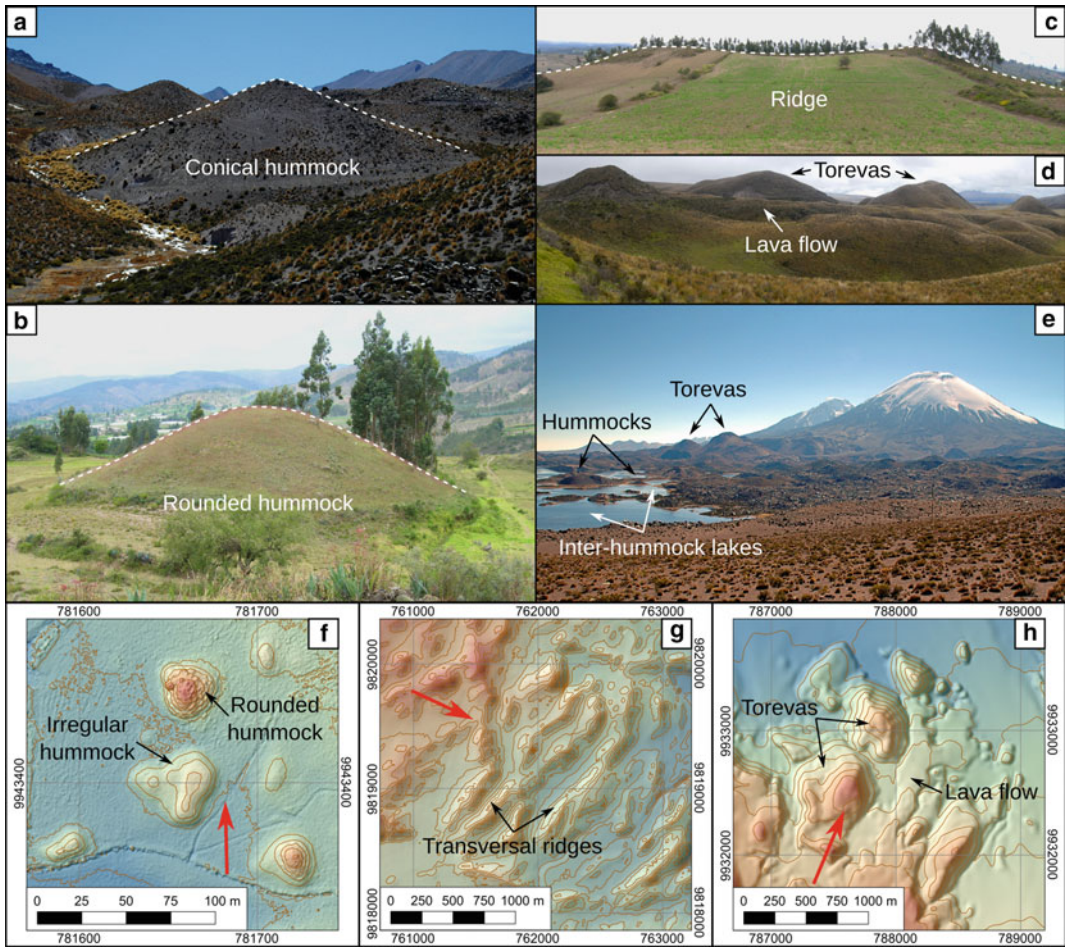

Fig. 9 Typical morphologies of the debris avalanche deposit topography. **a** Conical hummock from the proximal area of the 9–25 ka Taapaca VDAD (Chile). **b** Rounded hummock from the distal area of the 60–65 ka Chimborazo VDAD (Ecuador). **c** Ridge from the medial area of the 60–65 ka Chimborazo VDAD (Ecuador). **d** Torevas from the proximal area of the 4.5 ka Cotopaxi VDAD (Ecuador) with lava flow filling the inter-hummock depression. **E** Landscape of the proximal area of the 8 ka Parinacota VDAD (Chile). **f** Digital Elevation Model (DEM, 4 cm spatial resolution, 2 m isohypse interval) of rounded and irregular hummocks from the distal area of the 4.5 ka Cotopaxi VDAD (Ecuador). **g** DEM (4 m spatial resolution, 20 m isohypse interval) of transversal ridges from the medial area of the 60–65 ka Chimborazo VDAD (Ecuador). **h** DEM (4 m spatial resolution, 25 m isohypse interval) of torevas from the proximal area of the 4.5 ka Cotopaxi VDAD (Ecuador). Red arrows in the DEMs show the debris-avalanche direction

topography can be considerably modified by post-avalanche erosion and covering processes (Fig. 9e, h).

While the positive reliefs are commonly described, the depressions are often ignored. Inter-hummocks depressions are present between hummocks and might sometimes be filled by water (Fig. 9E). Furthermore, VDAD can present sub-circular depressions called “Kettle holes”, supposed to be left by the melting of large glacier blocks transported during the event (Glicken 1996; Clavero et al. 2002). Multiple grooves oriented parallel to the flow direction have also been observed in some cases, such as the 1964 Shiveluch VDAD (Belousov et al. 1999), the Pleistocene Llullaillaco VDAD (Richards and

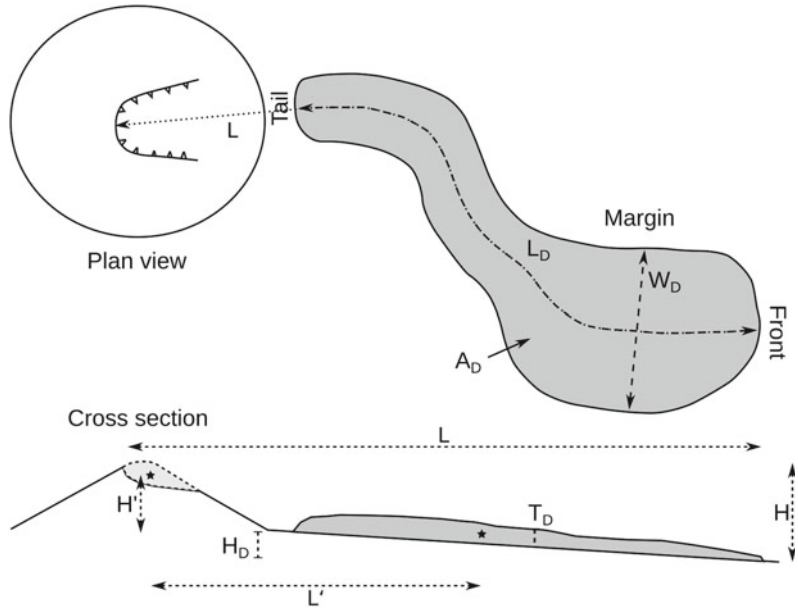

Fig. 10 Main descriptive terms and geometrical parameters for volcanic debris avalanche deposits defined in Table 3. Black stars: gravity center for the source and the deposit

Villeneuve 2001), and the 218 BP Tutupaca VDAD (Valderrama et al. 2016) and may be associated with granular fingering (Valderrama et al. 2018) or high-velocity emplacement (e.g., "herringbone" structures at Lastarria volcano; Naranjo and Francis 1987).

4.4 Metrics and Morphology

The deposit limits have not been formally named, and we, therefore, propose to use the term "front" for the distal limit, "margin" for the lateral sides of the deposit and "tail" for the proximal boundary (Fig. 5). It is possible to characterize the dimensions of the deposits and the transport phase with numerous geometrical parameters (Table 3). The deposit volume is a crucial parameter that can be estimated using different methods. Crandell et al. (1984) use the average thickness for seven different segments of the 300–380 ka Mount Shasta VDAD. Clavero et al. (2002) calculate the volume of hummocks of the 8 ka Parinacota VDAD to obtain a minimum value. For old deposits, it is necessary to reconstruct the pre-deposit topography. Erosion and covering of the VDAD induce large uncertainties in this calculation. Thus the volume obtained for old deposits may not be relevant. The measurement of the deposit area is generally much more reliable than volume estimates. Deposit shape parameters are poorly studied yet, but they can give valuable information on the transport constraints and the flow dynamics (Bernard 2008). When the geometries of the landslide scar and the debris avalanche deposit are well known, it is possible to quantify the transport phase (Fig. 10; Table 3).

So far, few studies have included the shape of the debris avalanche deposits in their description. However, some terms have appeared in the literature such as "fan-shaped" when unconfined with a large concave front (Siebert 2002; Bernard 2008), "wedged" when widest at the tail volcano and narrowing near the front (Clavero et al. 2002), "bifurcated" when the deposit is divided by a topographic obstacle (Richards and Villeneuve 2001), and "shoestring" or "elongated" when confined by valley walls (Siebert, 2002; Bernard 2008). The shape of the deposit can indicate if and how the debris avalanche was confined, which can affect its mobility (Bernard 2008).

Table 3 Definition of the quantitative parameters for the volcanic debris avalanche deposit

Acronym	Descriptive parameter	Definition
L_D	Deposit length	Distance between the front and the tail
W_D	Deposit width	Maximum distance between the deposit margins, orthogonal to the length
A_D	Deposit area	Surface covered by the deposit in plan view
H_D	Deposit height	Altitude difference between the tail and the front
α_D	Deposit declivity	Average slope between the tail and the front (α_D = atan H_D/L_D)
T_D[a]	Deposit thickness	Average thickness
V_D[a]	Deposit volume	Volume ($V_D = A_D \times T_D$)
AR_D	Deposit aspect ratio	Ratio between the average thickness and the radius of a circle of equal area ($AR_D = T_D/\sqrt{(A_D/\pi)}$)
L	Runout length	Distance between the scar head-wall and the deposit front. L′ is the distance between the gravity centers of the scar volume and the deposit volume (Heim 1932)
H	Drop height	Altitude difference between the maximum pre-landslide topography and the deposit front. H′ is the altitude difference between the gravity centers of the scar volume and the deposit volume (Heim 1932)
H/L	Apparent friction coefficient	Ratio between the drop height and runout length. H′/L′ is the true friction coefficient but might be complicated to obtain
SF	Spreading factor	Ratio between the deposit and the scar aspect ratios ($SF = AR_D/AR_S$)

[a]Parameters with a large error if pre- and/or post-avalanche topographies are poorly known

5 Conclusions

Four decades of research have increased our knowledge on volcanic landslides and debris avalanches, but, at the same time, the complexity of the scientific terminologies has also increased. Re-defining the key terms used to describe these phenomena and their geological features, coupled with a descriptive strategy, helps to standardize observations and enhance comparative analysis. The two main elements that indicate the occurrence of a volcanic landslide are the scar and the debris avalanche deposit. The volcanic landslide scars can be characterized using metrics, and their origin can be assessed through detailed geological observations. The description of volcanic debris avalanche deposits can be partitioned to obtain meaningful information on the emplacement mechanisms. Typical features are described and named, and the biggest challenge is now to produce a physical model that takes into account all the available data to fully understand the mobility of volcanic debris avalanches. Further analysis of their frequency, origin, and size are required to better understand and assess the associated hazard in volcanic settings.

Acknowledgements The authors thank Alexander Belousov and Mathieu Kervyn for their thoughtful reviews that helped improve the original manuscript. The authors also thank Lee Siebert for his help in clarifying some concepts and for being always open to discuss this topic. BB also acknowledges that this manuscript includes ideas he developed during its Ph.D. under the direction of Benjamin van Wyk de Vries, which is sincerely thanked.

References

Andrade SD, van Wyk de Vries B (2010) Structural analysis of the early stages of catastrophic stratovolcano flank-collapse using analogue models. Bull Volcanol 72:771–789. https://doi.org/10.1007/s00445-010-0363-x

Andrade SD, van Wyk de Vries B, Robin C (2018) Imbabura volcano (Ecuador): the influence of dipping-substrata on the structural development of composite volcanoes during strike-slip faulting. J Volcanol Geoth Res. https://doi.org/10.1016/j.jvolgeores.2018.11.017

Arce JL, Macías R, García Palomo A, Capra L, Macías JL, Layer P, Rueda H (2008) Late Pleistocene flank collapse of Zempoala volcano (Central Mexico) and the role of fault reactivation. J Volcanol Geoth Res 177:944–958. https://doi.org/10.1016/j.jvolgeores.2008.07.015

Auker MR, Sparks RSJ, Siebert L, Crosweller HS, Ewert J (2013) A statistical analysis of the global historical volcanic fatalities record. J Appl Volcanol 2:2. https://doi.org/10.1186/2191-5040-2-2

Belousov AB (1995) The Shiveluch volcanic eruption of 12 November 1964—explosive eruption provoked by failure of the edifice. J Volcanol Geoth Res 66:357–365. https://doi.org/10.1016/0377-0273(94)00072-O

Belousov A, Belousova M, Voight B (1999) Multiple edifice failures, debris avalanches and associated eruptions in the Holocene history of Shiveluch volcano, Kamchatka, Russia. Bull Volcanol 61:324–342. https://doi.org/10.1007/s004450050300

Bernard B (2008) Etude des dépôts d'avalanches de débris volcaniques: analyse sédimentologiques d'exemples naturels et identification des mécanismes de mise en place. Ph.D. thesis. Université Blaise Pascal, Clermont-Ferrand II, 293p

Bernard B, Andrade SD (2019) Large volcanic debris avalanches in Ecuador. In: Abstract volume of the 8th international symposium on Andean geodynamics. Quito, Ecuador

Bernard B, van Wyk de Vries B (2010) Incorporation processes in volcanic rockslide-debris avalanches from field observations: implications on emplacement mechanisms. In: Geophysical research abstracts. EGU2010-6643

Bernard B, van Wyk de Vries B, Barba D, Leyrit H, Robin C, Alcaraz S, Samaniego P (2008) The Chimborazo sector collapse and debris avalanche: deposit characteristics as evidence of emplacement mechanisms. J Volcanol Geoth Res 176:36–43. https://doi.org/10.1016/j.jvolgeores.2008.03.012

Bernard B, Wyk V, de Vries B, Leyrit H (2009) Distinguishing volcanic debris avalanche deposits from their reworked products: the Perrier sequence (French Massif Central). Bull Volcanol 71:1041–1056. https://doi.org/10.1007/s00445-009-0285-7

Bernard B, Robin C, Beate B, Hidalgo S (2011) Nuevo modelo evolutivo y actividad eruptiva reciente del volcán Chachimbiro. In: Libro de resúmenes extendidos de las 7mas Jornadas en Ciencias de la Tierra. Quito, Ecuador

Boudon G, Semet MP, Vincent PM (1987) Magma and hydrothermally driven sector collapses: The 3100 and 11,500 y. B.P. eruptions of la Grande Decouverte (la Soufrière) volcano, Guadeloupe, French West Indies. J Volcanol Geoth Res 33:317–323. https://doi.org/10.1016/0377-0273(87)90021-7

Capra L, Macías JL (2000) Pleistocene cohesive debris flows at Nevado de Toluca Volcano, central Mexico. J Volcanol Geoth Res 102:149–167. https://doi.org/10.1016/S0377-0273(00)00186-4

Capra L, Macías JL, Scott KM, Abrams M, Garduño-Monroy VH (2002) Debris avalanches and debris flows transformed from collapses in the Trans-Mexican Volcanic Belt, Mexico—behavior, and implications for hazard assessment. J Volcanol Geoth Res 113:81–110. https://doi.org/10.1016/S0377-0273(01)00252-9

Carracedo JC, Day SJ, Guillou H, Pérez Torrado FJ (1999) Giant quaternary landslides in the evolution of La Palma and El Hierro, Canary Islands. J Volcanol Geoth Res 94:169–190. https://doi.org/10.1016/S0377-0273(99)00102-X

Cas RA, Wright JV (1987) Volcanic successions: modern and ancient—a geological approach to processes, products and successions. Chapman and Hall, London, p 528

Clavero J, Sparks R, Huppert H, Dade W (2002) Geological constraints on the emplacement mechanism of the Parinacota debris avalanche, Northern Chile. Bull Volcanol 64:40–54. https://doi.org/10.1007/s00445-001-0183-0

Clavero JE, Sparks RSJ, Pringle MS, Polanco E, Gardeweg MC (2004) Evolution and volcanic hazards of Taapaca volcanic complex, Central Andes of Northern Chile. J Geol Soc 161:603–618. https://doi.org/10.1144/0016-764902-065

Conway MF, Vallance JW, Rose WI, Johns GW, Paniagua S (1992) Cerro Quemado, Guatemala: the volcanic history and hazards of an exogenous volcanic dome complex. J Volcanol Geoth Res 52:303–323. https://doi.org/10.1016/0377-0273(92)90051-E

Coombs ML, White SM, Scholl DW (2007) Massive edifice failure at Aleutian arc volcanoes. Earth Planet Sci Lett 256:403–418. https://doi.org/10.1016/j.epsl.2007.01.030

Crandell DR, Miller CD, Glicken HX, Christiansen RL, Newhall CG (1984) Catastrophic debris avalanche from ancestral Mount Shasta volcano, California. Geology 12:143–146. https://doi.org/10.1130/0091-7613(1984)12%3c143:CDAFAM%3e2.0.CO;2

Crosta GB, Imposimato S, Roddeman D, Chiesa S, Moia F (2005) Small fast-moving flow-like landslides in volcanic deposits: the 2001 Las Colinas Landslide (El Salvador). Eng Geol 79:185–214. https://doi.org/10.1016/j.enggeo.2005.01.014

Cruden DM, Lu ZY (1992) The rockslide and debris flow from Mount Cayley, BC, in June 1984. Can Geotech J 29:614–626. https://doi.org/10.1139/t92-069

Day SJ, Carracedo JC, Guillou H (1997) Age and geometry of an aborted rift flank collapse: the San Andres fault system, El Hierro, Canary Islands. Geol Mag 134:523–537. https://doi.org/10.1017/S0016756897007243

Day SJ, Heleno Da Silva SIN, Fonseca JFBD (1999) A past giant lateral collapse and present-day flank instability of Fogo, Cape Verde Islands. J Volcanol Geoth Res 94:191–218. https://doi.org/10.1016/S0377-0273(99)00103-1

Delcamp A, Delvaux D, Kwelwa S, Macheyeki A, Kervyn M (2016) Sector collapse events at volcanoes in the North Tanzanian divergence zone and their implications for regional tectonics. Bull Geol Soc Am 128:169–186. https://doi.org/10.1130/B31119.1

Delcamp A, Kervyn M, Benbakkar M, Kwelwa S, Peter D (2017) Large volcanic landslide and debris avalanche deposit at Meru, Tanzania. Landslides 14:833–847. https://doi.org/10.1007/s10346-016-0757-8

Duffield WA, Stieltjes L, Varet J (1982) Huge landslide blocks in the growth of piton de la fournaise, La réunion, and Kilauea volcano, Hawaii. J Volcanol Geoth Res 12:147–160. https://doi.org/10.1016/0377-0273(82)90009-9

Dufresne A (2009) Influence of runout path material on rock and debris avalanche mobility: field evidence and analogue modelling. Ph.D. thesis. University of Canterbury, New Zealand, 268p

Dufresne A, Davies TR (2009) Longitudinal ridges in mass movement deposits. Geomorphology 105:171–181. https://doi.org/10.1016/j.geomorph.2008.09.009

Dufresne A, Salinas S, Siebe C (2010) Substrate deformation associated with the Jocotitlán edifice collapse and debris avalanche deposit, Central México. J Volcanol Geoth Res 197:133–148. https://doi.org/10.1016/j.jvolgeores.2010.02.019

Dufresne A, Bösmeier A, Prager C (2016) Sedimentology of rock avalanche deposits—case study and review. Earth Sci Rev 163:234–259. https://doi.org/10.1016/j.earscirev.2016.10.002

Dufresne A, Zernack AV, Bernard K, Thouret J-C, Roverato M (2020) Sedimentology of volcanic debris avalanche deposits. In: Roverato M, Dufresne A, Procter JN (eds) Volcanic debris avalanches: from collapse to Hazard. Springer book series advances in volcanology (this volume)

Elsworth D, Day SJ (1999) Flank collapse triggered by intrusion: the Canarian and cape verde archipelagoes. J Volcanol Geoth Res 94:323–340. https://doi.org/10.1016/S0377-0273(99)00110-9

Encalada M, Bernard B (2018) Dynamics of Cotopaxi volcano debris avalanche. In: Abstract volume of the international meeting cities on Volcanoes, vol 10. Naples, Italy, p 682

Fisher RV, Glicken HX, Hoblitt RP (1987) May 18, 1980, Mount St. Helens deposits in South Coldwater Creek, Washington. J Geophys Res Solid Earth 92:10267–10283. https://doi.org/10.1029/JB092iB10p10267

Friedmann SJ (1997) Rock-avalanche elements of the Shadow Valley basin, eastern Mojave Desert, California; processes and problems. J Sediment Res 67:792–804. https://doi.org/10.1306/D426863F-2B26-11D7-8648000102C1865D

Glicken H (1991) Sedimentary architecture of large volcanic-debris avalanches. In: Fisher RV, Smith GA (eds) Sedimentation in volcanic settings. Special publication. SEPM, pp 99–106. https://doi.org/10.2110/pec.91.45.0099

Glicken H (1996) Rockslide-debris avalanche of May 18, 1980, Mount St. Helens volcano, Washington. U.S. geological survey open-file report 96-677, 90p, 5 plates, https://pubs.usgs.gov/of/1996/0677/

Grab S (2005) Aspects of the geomorphology, genesis and environmental significance of earth hummocks (thúfur, pounus): miniature cryogenic mounds. Progr Phys Geogr Earth Environ 29:139–155. https://doi.org/10.1191/0309133305pp440ra

Hayashi JN, Self S (1992) A comparison of pyroclastic flow and debris avalanche mobility. J Geophys Res 97:9063–9071. https://doi.org/10.1029/92JB00173

Heim A (1932) Bergsturz und Menschenleben. Fretz & Wasmuth, 218 p

Hungr O, Leroueil S, Picarelli L (2014) The Varnes classification of landslide types, an update. Landslides 11:167–194. https://doi.org/10.1007/s10346-013-0436-y

Hürlimann M, Garcia-Piera JO, Ledesma A (2000) Causes and mobility of large volcanic landslides: application to Tenerife, Canary Islands. J Volcanol Geoth Res 103:132–134. https://doi.org/10.1016/S0377-0273(00)00219-5

Iverson RM (1995) Can magma-injection and groundwater forces cause massive landslides on Hawaiian volcanoes? J Volcanol Geoth Res 66:295–308. https://doi.org/10.1016/0377-0273(94)00064-N

Johnson RW (1987) Large-scale volcanic cone collapse: The 1888 slope failure of Ritter volcano, and other examples from Papua New Guinea. Bull Volcanol 49:669–679. https://doi.org/10.1007/BF01080358

Karátson D, Thouret J-C, Moriya I, Lomoschitz A (1999) Erosion calderas: origins, processes, structural and climatic control. Bull Volcanol 61:174–193. https://doi.org/10.1007/s004450050270

Kelfoun K, Druitt T, van Wyk de Vries B, Guilbaud M-N (2008) Topographic reflection of the Socompa debris avalanche, Chile. Bull Volcanol 70:1169–1187. https://doi.org/10.1007/s00445-008-0201-6

Kerle N, van Wyk de Vries B (2001) The 1998 debris avalanche at Casita Volcano, Nicaragua—investigation of structural deformation as the cause of slope instability using remote sensing. J Volcanol Geoth Res 105:49–63. https://doi.org/10.1016/S0377-0273(00)00244-4

Kervyn M, Ernst GGJ, Klaudius J, Keller J, Mbede E, Jacobs P (2008) Remote sensing study of sector collapses and debris avalanche deposits at Oldoinyo Lengai and Kerimasi volcanoes, Tanzania. Int J Remote Sens 29:6565–6595. https://doi.org/10.1080/01431160802168137

Kokelaar P, Romagnoli C (1995) Sector collapse, sedimentation and clast population evolution at an active island-arc volcano: Stromboli, Italy. Bull Volcanol 57:240–262. https://doi.org/10.1007/BF00265424

Komorowski J-C, Glicken HX, Sheridan MF (1991) Secondary electron imagery of microcracks and hackly fracture surfaces in sand-size clasts from the 1980 Mount St. Helens debris- avalanche deposit: implications for particle-particle interactions. Geology 19:261–264. https://doi.org/10.1130/0091-7613(1991)019%3c0261:SEIOMA%3e2.3.CO;2

Lagmay AMF, van Wyk De Vries B, Kerle N, Pyle DM (2000) Volcano instability induced by strike-slip faulting. Bull Volcanol 62:331–346. https://doi.org/10.1007/s004450000103

Le Friant A, Harford C, Deplus C, Boudon G, Sparks S, Herd R, Komorowski JC (2004) Geomorphological

evolution of Montserrat (West Indies): importance of flank collapse and erosional processes. J Geol Soc London 161:147–160. https://doi.org/10.1144/0016-764903-017

Legros F (2002) The mobility of long-runout landslides. Eng Geol 63:301–331. https://doi.org/10.1016/S0013-7952(01)00090-4

Legros F, Cantagrel J-M, Devouard B (2000) Pseudotachylyte (frictionite) at the base of the Arequipa volcanic landslide deposit (Peru): implications for emplacement mechanisms. J Geol 108:601–611. https://doi.org/10.1086/314421

Leyrit H (2000) Flank collapse and debris avalanche deposits. In: Leyrit H, Montenat C (eds) Volcaniclastic rocks, from magmas to sediments. Gordon and Breach Science Publishers, pp 111–129

Lipman PW, Moore JG, Swanson DA (1981) Bulging of the north flank before the May 18 eruption-geodetic data. In: Lipman PW, Mulineaux DR (eds) The 1980 eruptions of Mount St. Helens, Washington. US geological survey professional paper, vol 1250, pp 631–639

Lipman PW, Eakins BW, Yokose H (2003) Ups and downs on spreading flanks of ocean-island volcanoes: evidence from Mauna Loa and Kīlauea. Geology 31:841–844. https://doi.org/10.1130/G19745.1

Macías JL, Arce JL, García-Palomo A, Mora JC, Layer PW, Espíndola JM (2010) Late-Pleistocene flank collapse triggered by dome growth at Tacaná volcano, México-Guatemala, and its relationship to the regional stress regime. Bull Volcanol 72:33–53. https://doi.org/10.1007/s00445-009-0303-9

Marti J, Hurlimann M, Abley GJ, Gudmundsson A (1997) Vertical and lateral collapses on Tenerife (Canary Islands) and other volcanic ocean islands. Geology 25:879–882. https://doi.org/10.1130/0091-7613(1997)025%3c0879:VALCOT%3e2.3.CO;2

McEwen AS, Malin MC (1989) Dynamics of Mount St. Helens' 1980 pyroclastic flows, rockslide-avalanche, lahars, and blast. J Volcanol Geoth Res 37:205–231. https://doi.org/10.1016/0377-0273(89)90080-2

McGuire WJ (1996) Volcano instability: a review of contemporary themes. In: McGuire WJ, Jones AP, Neuberg J (eds) Volcano instability on the Earth and other planets. Geological Society, London, pp 1–23

McSaveney MJ, Davies TR, Hodgson KA (2000) A contrast in deposit style and process between large and small rock avalanches. In: Bromhead E, Dixon N, Ibsen ML (eds) Landslides in research, theory and practice. In: Proceedings 8th international symposium on landslides. Thomas Telford, Cardiff, 26–30 June 2000, pp 1052–1058

Mehl KW, Schmincke H-U (1999) Structure and emplacement of the Pliocene Roque Nublo debris avalanche deposit, Gran Canaria, Spain. J Volcanol Geoth Res 94:105–134. https://doi.org/10.1016/S0377-0273(99)00100-6

Naranjo JA, Francis P (1987) High velocity debris avalanche at Lastarria volcano in the north Chilean Andes. Bull Volcanol 49:509–514. https://doi.org/10.1007/BF01245476

Nehlig P, Leyrit H, Dardon A, Freour G, de Herve A, de G, Huguet D, Thieblemont D (2001) Constructions et destructions du stratovolcan du Cantal. Bull Soc Geol Fr 172:295–308. https://doi.org/10.2113/172.3.295

Oehler J-F, Lénat J-F, Labazuy P (2008) Growth and collapse of the Reunion Island volcanoes. Bull Volcanol 70:717–742. https://doi.org/10.1007/s00445-007-0163-0

Ozeki N, Okuno M, Kobayashi T (2005) Growth history of Mayuyama, Unzen Volcano, Kyushu, southwest Japan. Bull Volcanol Soc Japan 50:441–454

Paguican EMR, van Wyk de Vries B, Lagmay AMF (2012) Volcano-tectonic controls and emplacement kinematics of the Iriga debris avalanches (Philippines). Bull Volcanol 74:2067–2081. https://doi.org/10.1007/s00445-012-0652-7

Paguican EMR, van Wyk de Vries B, Lagmay AMF (2014) Hummocks: how they form and how they evolve in rockslide-debris avalanches. Landslides 11:67–80. https://doi.org/10.1007/s10346-012-0368-y

Palmer BA, Alloway BV, Neall VE (1991) Volcanic-debris-avalanche deposits in New Zealand - lithofacies organization in unconfined, wet-avalanche flows. In: Fisher RV, Smith GA (eds) Sedimentation in volcanic settings. Special publication SEPM, pp 89–98. https://doi.org/10.2110/pec.91.45.0089

Paris R, Carracedo JC (2001) Formation d'une caldera d'érosion et instabilité récurrente d'une île de point chaud: la caldera de Taburiente, La Palma, îles Canaries/Formation of an erosion caldera and recurring instability on a hotspot-generated island: the caldera de Taburiente, La Palma, Canary Islands. Géomorphol Relief Process Environ 7:93–105. https://doi.org/10.3406/morfo.2001.1093

Paris R, Giachetti T, Chevalier J, Guillou H, Frank N (2011) Tsunami deposits in Santiago Island (Cape Verde archipelago) as possible evidence of a massive flank failure of Fogos volcano. Sed Geol 239:129–145. https://doi.org/10.1016/j.sedgeo.2011.06.006

Petley DN, Allison RJ (1997) The mechanics of deep-seated landslides. Earth Surf Proc Land 22:747–758. https://doi.org/10.1002/(SICI)1096-9837(199708)22:8%3c747::AID-ESP767%3e3.0.CO;2-#

Ponomareva VV, Melekestsev IV, Dirksen OV (2006) Sector collapses and large landslides on Late Pleistocene-Holocene volcanoes in Kamchatka, Russia. J Volcanol Geoth Res 158:117–138. https://doi.org/10.1016/j.jvolgeores.2006.04.016

Reiche P (1937) The toreva block—a distinctive landslide type. J Geol 45:538–548

Richards JP, Villeneuve M (2001) The Llullaillaco Volcano, northwest Argentina: construction by Pleistocene volcanism and destruction by sector collapse. J Volcanol Geoth Res 105:77–105. https://doi.org/10.1016/S0377-0273(00)00245-6

Riggs N, Carrasco-Nunez G (2004) Evolution of a complex isolated dome system, Cerro Pizarro, central

México. Bull Volcanol 66:322–335. https://doi.org/10.1007/s00445-003-0313-y

Roa K (2003) Nature and origin of toreva remnants and volcaniclastics from La Palma, Canary Islands. J Volcanol Geoth Res 125:191–214. https://doi.org/10.1016/S0377-0273(03)00069-6

Robin C, Samaniego P, Le Pennec J-L, Fornari M, Mothes P, van der Plicht J (2010) New radiometric and petrological constraints on the evolution of the Pichincha volcanic complex (Ecuador). Bull Volcanol 72(9):1109–1129. https://doi.org/10.1007/s00445-010-0389-0

Romagnoli C, Casalbore D, Chiocci FL, Bosman A (2009) Offshore evidence of large-scale lateral collapses on the eastern flank of Stromboli, Italy, due to structurally-controlled, bilateral flank instability. Mar Geol 262:1–13. https://doi.org/10.1016/j.margeo.2009.02.004

Roverato M, Capra L, Sulpizio R, Norini G (2011) Stratigraphic reconstruction of two debris avalanche deposits at Colima Volcano (Mexico): insights into pre-failure conditions and climate influence. J Volcanol Geoth Res 207:33–46. https://doi.org/10.1016/j.jvolgeores.2011.07.003

Roverato M, Cronin S, Procter J, Capra L (2015) Textural features as indicators of debris avalanche transport and emplacement, Taranaki volcano. GSA Bull 127:3–18

Roverato M, Di Traglia F, Procter JN, Paguican EMR, Dufresne A (2020) Factors contributing to volcano lateral collapse. In: Roverato M, Dufresne A, Procter JN (eds) Volcanic debris avalanches: from Collapse to Hazard. Springer book series advances in volcanology (this volume)

Schneider J-L, Fisher RV (1998) Transport and emplacement mechanisms of large volcanic debris avalanches: evidence from the northwest sector of Cantal Volcano (France). J Volcanol Geoth Res 83:141–165. https://doi.org/10.1016/S0377-0273(98)00016-X

Scott KM, Vallance JW, Kerle N, Macías JL, Strauch W, Devoli G (2005) Catastrophic precipitation-triggered lahar at Casita volcano, Nicaragua: Occurrence, bulking and transformation. Earth Surf Proc Land 30:59–79. https://doi.org/10.1002/esp.1127

Shea T, van Wyk de Vries B (2008) Structural analysis and analogue modeling of the kinematics and dynamics of rockslide avalanches. Geosphere 4:657–686. https://doi.org/10.1130/GES00131.1

Shea T, van Wyk de Vries B, Pilato M (2008) Emplacement mechanisms of contrasting debris avalanches at Volcán Mombacho (Nicaragua), provided by structural and facies analysis. Bull Volcanol 70:899–921. https://doi.org/10.1007/s00445-007-0177-7

Siebert L (1984) Large volcanic debris avalanches: Characteristics of source areas, deposits, and associated eruptions. J Volcanol Geoth Res 22:163–197. https://doi.org/10.1016/0377-0273(84)90002-7

Siebert L (2002) Landslides resulting from structural failure of volcanoes. Rev Eng Geol 15:209–235. https://doi.org/10.1130/REG15-p209

Siebert L, Roverato M (2020) A historical perspective on lateral collapse and debris avalanches. In: Roverato M, Dufresne A, Procter J (eds) Volcanic dedris avalanches: from collapse to hazard, advances in volcanology. Springer

Siebert L, Glicken H, Ui T (1987) Volcanic hazards from Bezymianny- and Bandai-type eruptions. Bull Volcanol 49:435–459. https://doi.org/10.1007/BF01046635

Siebert L, Kimberly P, Pullinger CR (2004) The voluminous Acajutla debris avalanche from Santa Ana volcano, western El Salvador, and comparison with other Central American edifice-failure events. In: Special paper 375: Natural hazards in El Salvador. Geological Society of America, pp 5–24. https://doi.org/10.1130/0-8137-2375-2.5

Stoffel DB, Stoffel KL (1980) Mt. St. Helens close up on May 18. Geotimes 25:16–17

Stoopes GR, Sheridan MF (1992) Giant debris avalanches from the Colima Volcanic Complex, Mexico: implications for long-runout landslides (>100 km) and hazard assessment. Geology 20:299–302. https://doi.org/10.1130/0091-7613(1992)020%3c0299:GDAFTC%3e2.3.CO;2

Strasser M, Schlunegger F (2005) Erosional processes, topographic length-scales and geomorphic evolution in arid climatic environments: the 'Lluta collapse', northern Chile. Int J Earth Sci 94:433–446. https://doi.org/10.1007/s00531-005-0491-2

Takarada S, Ui T, Yamamoto Y (1999) Depositional features and transportation mechanism of valley-filling Iwasegawa and Kaida debris avalanches, Japan. Bull Volcanol 60:508–522. https://doi.org/10.1007/s004450050248

Tibaldi A, Bistacchi A, Pasquarè FA, Vezzoli L (2006) Extensional tectonics and volcano lateral collapses: Insights from Ollagüe volcano (Chile-Bolivia) and analogue modelling. Terra Nova 18:282–289. https://doi.org/10.1111/j.1365-3121.2006.00691.x

Ui T (1983) Volcanic dry avalanche deposits—identification and comparison with nonvolcanic debris stream deposits. J Volcanol Geoth Res 18:135–150. https://doi.org/10.1016/0377-0273(83)90006-9

Ui T, Glicken H (1986) Internal structural variations in a debris-avalanche deposit from ancestral Mount Shasta, California, USA. Bull Volcanol 48:189–194. https://doi.org/10.1007/BF01087673

Ui T, Yamamoto H, Suzuki-Kamata K (1986) Characterization of debris avalanche deposits in Japan. J Volcanol Geoth Res 29:231–243. https://doi.org/10.1016/0377-0273(86)90046-6

Ui T, Takarada S, Yoshimoto M (2000) Debris avalanches. In: Sigurdsson H, Houghton B, McNutt SR, Rymer H, Stix J (eds) Encyclopedia of volcanoes. Academic Press, London, pp 617–626

Valderrama P, Roche O, Samaniego P, van Wyk de Vries B, Bernard K, Mariño J (2016) Dynamic implications of ridges on a debris avalanche deposit at Tutupaca volcano (southern Peru). Bull Volcanol 78:1–11. https://doi.org/10.1007/s00445-016-1011-x

Valderrama P, Roche O, Samaniego P, van Wyk des Vries B, Araujo G (2018) Granular fingering as a mechanism for ridge formation in debris avalanche

deposits: laboratory experiments and implications for Tutupaca volcano, Peru. J Volcanol Geoth Res 349: 409–418. https://doi.org/10.1016/j.jvolgeores.2017.12.004

van Wyk de Vries B, Delcamp A (2015) Volcanic debris avalanches. In: Shroder JF, Davies T (eds) Landslide hazards, risks, and disasters. Academic Press. pp 131–157. https://doi.org/10.1016/B978-0-12-396452-6.00005-7

van Wyk de Vries B, Self S, Francis PW, Keszthelyi L (2001) A gravitational spreading origin for the Socompa debris avalanche. J Volcanol Geoth Res 105:225–247. https://doi.org/10.1016/S0377-0273(00)00252-3

Varnes DJ (1978) Slope movement types and processes. Landslides Anal Control 176:11–33

Vincent PM, Bourdier JL, Boudon G (1989) The primitive volcano of Mount Pelée: its construction and partial destruction by flank collapse. J Volcanol Geoth Res 38:1–15. https://doi.org/10.1016/0377-0273(89)90026-7

Voight B, Glicken H, Janda RJ, Douglass M (1981) Catastrophic rockslide avalanche of May 18 (Mount St. Helens). In: Lipman PW, Mulineaux DR (eds) The 1980 eruptions of Mount St. Helens, Washington. US geological survey professional paper, vol 1250, pp 347–377

Voight B, Komorowski J-C, Norton GE, Belousov AB, Belousova M, Boudon G, Francis PW, Franz W, Heinrich P, Sparks RSJ, Young SR (2002) The 26 December (Boxing Day) 1997 sector collapse and debris avalanche at Soufrière Hills Volcano, Montserrat. Geol Soc Mem 21:363–407. https://doi.org/10.1144/GSL.MEM.2002.021.01.17

Watt SFL, Pyle DM, Naranjo JA, Mather TA (2009) Landslide and tsunami hazard at Yate volcano, Chile as an example of edifice destruction on strike-slip fault zones. Bull Volcanol 71:559–574. https://doi.org/10.1007/s00445-008-0242-x

Williams R, Rowley P, Garthwaite MC (2019) Reconstructing the Anak Krakatau flank collapse that caused the December 2018 Indonesian tsunami. EarthArXiv. https://doi.org/10.31223/osf.io/u965c

Yarnold JC (1993) Rock-avalanche characteristics in dry climates and the effect of flow into lakes: insights from mid-Tertiary sedimentary breccias near Artillery Peak, Arizona. Geol Soc Am Bull 105:345–360. https://doi.org/10.1130/0016-7606(1993)105%3c0345:RACIDC%3e2.3.CO;2

Yoshida H (2016) Magnitude-frequency distribution of hummocks on rockslide-debris avalanche deposits and its geomorphological significance. Geosci (Switz) 6. https://doi.org/10.3390/geosciences6010005

Yoshida H, Sugai T (2007) Magnitude of the sediment transport event due to the Late Pleistocene sector collapse of Asama volcano, central Japan. Geomorphology 86:61–72. https://doi.org/10.1016/j.geomorph.2006.08.006

Yoshimatsu H, Abe S (2006) A review of landslide hazards in Japan and assessment of their susceptibility using an analytical hierarchic process (AHP) method. Landslides 3:149–158. https://doi.org/10.1007/s10346-005-0031-y